NRC Publications Archive
Archives des publications du CNRC

Optical coherence tomography for industrial and biomedical applications

Lamouche, Guy; Bisaillon, Charles-Etienne; Dufour, Marc; Gauthier, Bruno; Maciejko, Romain; Monchalin, Jean-Pierre

NRC Publications Record / Notice d'Archives des publications de CNRC:
https://nrc-publications.canada.ca/eng/view/object/?id=7a14cca7-535d-4067-b906-fae65b10e954
https://publications-cnrc.canada.ca/fra/voir/objet/?id=7a14cca7-535d-4067-b906-fae65b10e954

National Research Council Canada   Conseil national de recherches Canada

Canada

Optical coherence tomography for industrial and biomedical applications

Guy Lamouche[a], Charles-Etienne Bisaillon[a,b], Marc Dufour[a], Bruno Gauthier[a], Romain Maciejko[b], and Jean-Pierre Monchalin*[a]

[a]Institut des matériaux industriels, Conseil national de recherches Canada, 75 de Mortagne, Boucherville, Québec,Canada, J4B 6Y4

[b]Laboratoire d'optoélectronique, Département de génie physique, Ecole Polytechnique de Montréal, P.O. Box 6079, Station "Centre-ville" Montréal, Québec, Canada H3C 3A7

ABSTRACT

An overview of the activities in low-coherence interferometry (LCI) and optical coherence tomography (OCT) at the Industrial Materials Institute are presented. An innovative optical delay line using rhombic prisms is described. A few industrial applications are described: volume loss in a wear test, combination of LCI with laser-induced breakdown spectroscopy, and modification of an existing rheometer to increase its precision. Preliminary results related to the use of speckle to differentiate tissues and materials in OCT are presented. The speckle dimension is shown to be sensitive to low density of scatterers. An additional parameter extracted from the autocorrelation of speckle is also presented.

Keywords: Optical coherence tomography, delay line, speckle

1. INTRODUCTION

The Industrial Materials Institute (IMI) has been active for many years in the field of low-coherence interferometry (LCI) initially to perform profilometry for industrial applications and later to perform optical coherence tomography (OCT) for both industrial and biomedical applications. In this paper, we provide an overview of these activities at IMI. We begin in Section 2 with a glimpse at the basic technology developed at IMI by describing an efficient optical delay line to use as a basis of an LCI system or a time-domain OCT system. Our technology relies on rotating rhombic prisms and uses reinjection of light, resulting in a delay line that is robust and easy to align while providing good linearity and high duty cycle. In Section 3, we briefly describe various industrial and biomedical applications for which our technology has provided efficient solutions. In Section 4, we present some preliminary work related to the use of speckle to differentiate biological tissues or industrial materials, a collaborative effort with Ecole Polytechnique of Montreal.

2. OPTICAL DELAY LINE

Optical coherence tomography is now an established technique for cross-sectional imaging in biomedical applications. Although the technique is full of potential for industrial applications, only few realizations have been achieved in this latter field. A typical time-domain OCT system contains a sample arm in which the volume of a sample is illuminated with a broadband source and the backscattered light is collected and made to interfere with that from a reference arm. The reference arm contains an optical delay line to continuously vary the depth at which the sample is probed. The development of optical delay lines has been a quite active field during the last decade, especially for time-domain OCT where one is striving for high measurement rates to achieve real-time imaging. Important parameters for optical delay lines are: scan range, scan velocity, duty cycle, linearity, dispersion and polarization effects. For the mass production of optical delay lines and for continuous use in medical or industrial environments, there are two important additional criteria often less considered: the ease of optical alignment and the robustness of the delay line.

OCT measurements are generally performed with a scan range of a few millimeters and require a repetition rate of at least a few kilohertz to allow real-time imaging. A detailed review of optical delay lines used in OCT has been published

*jean-pierre.monchalin@cnrc-nrc.gc.ca; phone 1 450 641-5122; fax 1 450 641-5116; www.imi.nrc.ca

by Rollins and Izatt[1]. The simplest designs rely on the translation of a retroreflective element or on galvanometer-mounted retroreflectors. These generally suffer from low scanning repetition rate and nonlinearity. Higher stability and higher repetition rates can be obtained from uniformly rotating elements. Many designs were proposed based on this approach and these suffer to various degrees from one or many of the following: low-duty cycle, nonlinearity, difficult alignment, and lack of robustness. A celebrated approach based on the use of a grating was first proposed by Kwong et al.[2] and later improved by Tearney et al.[3]. Although elegant, this design is quite delicate to handle.

Initial work at IMI was performed with a galvanometer mounted optical element. Since then, IMI has developed an innovative optical delay line that relies on the use of an ensemble of rhombic prisms on a rotating disc with reinjection of light. A specific realization of the setup is illustrated in Fig. 1a where five rhombic prisms are symmetrically placed around a disc. Light exiting the optical coupler is directed towards one prism where it is internally reflected twice to exit parallel to its initial direction. It is then retroreflected by a mirror to follow the exact inverse path to be collected by the optical coupler. The total optical path length varies with the orientation of the prism as the ensemble rotates. During a full rotation, all five prisms intercept the light for a given angular range that corresponds to about 36° in Fig. 1a. When light is not directly intercepted by one of the prism, it can be redirected with the use of a mirror as in Fig.1b. With this re-injection, all prisms are used twice over a single rotation, thus increasing the duty cycle.

The rhombic prism is a very forgiving optical element since it can be used even when slightly misoriented. An optical delay line using rhombic prisms is thus very easy to align and quite robust. By having the ensemble of prisms on a rotating disc, one can obtain a stable and high repetition rate with commercially available high-speed rotating motors. Additionally, by using reinjection of the optical ray and by wisely positioning and orienting the prisms on the rotating disc, one can obtain good linearity and high duty cycle. For example, with rhombic prisms with a side dimension of 3 mm, one can obtain variation of 2.6 mm in optical pathlength, a duty cycle exceeding 90% and a nonlinearity that amounts to 6%. Current IMI system is providing 4000 delay scans per second, but higher scan rates are achievable. This technology is patent pending and available through Novacam Technologies (www.novacam.com).
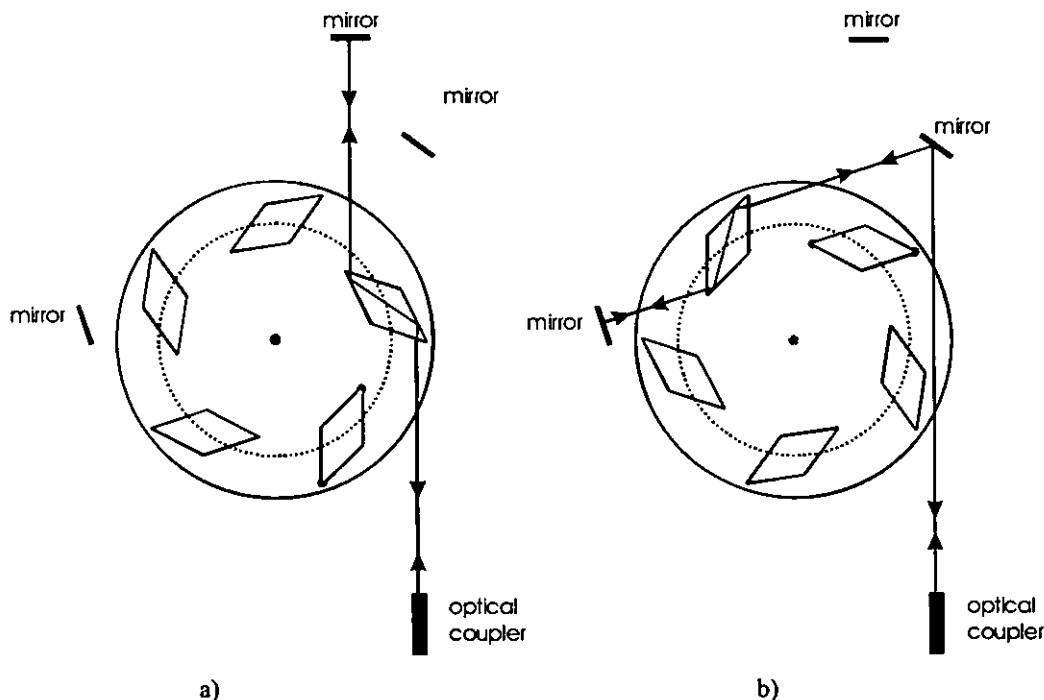

a)   b)

Fig. 1. Optical delay line based on five rhombic prisms rotating on a disc. Figure 1a illustrates the case were light is directly intercepted by a prism. In Figure 1b, the ensemble is rotated and a mirror is used to insure reinjection of light in the ensemble, thus doubling the duty cycle.

3. INDUSTRIAL APPLICATIONS

Many of the early use of OCT were targeting ophthalmology, but OCT now covers a wide range of topics in biomedical applications. The goal of this section is to review some applications developed at IMI illustrating that the underlying technology for LCI and OCT is also well suited to industrial applications. These applications are discussed more at length in Ref. 4.

First example relates to the use of LCI to perform precise profilometry. When the sample presents a well-defined interface, a resolution smaller than a micron can be obtained even with a superluminescent source with a coherence length in the tens of microns since the center of the envelope function of the interferogram can be precisely determined. One such application developed at IMI is volume loss determination in a wear test. A surface map is obtained by scanning LCI measurements over the damaged region. The scanned surface must exceed the damaged region since an intact surface around it is necessary for reference purpose. The volume loss is evaluated by first determining the reference profile corresponding to an intact region. For such measurements, the required transverse resolution is not too severe. But the resolution in depth (axial resolution) must be of the order of a micron since the maximum depth measured in a wear test may be as small as 10 microns. IMI developed a robust and low-cost prototype for this application. Our first client was our Surface Technologies group who has successfully used the system for more than 6 years. A system was also delivered to Syncrude Canada Ltd.

The technology underlying LCI and OCT is quite easily combined with other techniques to provide multimodal instrumentation. An example for OCT in biomedical applications is the combination of OCT and fluorescence imaging. IMI has combined LCI interferometry with laser induced breakdown spectroscopy (LIBS). LIBS is a powerful technique for rapid on-site analysis of solid, liquid, or gas. In LIBS, a powerful laser beam is focused on a sample, vaporizing some matter and creating a plasma. Light emitted by this plasma is spectrally analyzed to identify elements, the intensity of the lines providing quantitative concentration measurements usually down to one ppm. For a solid sample, each LIBS laser shot removes some material and digs a small hole in the sample. LCI is used to measure the depth of the crater. The LCI-LIBS combination allows the measurement of the concentration as a function of depth in a sample.

The technology is versatile enough to be combined with existing equipment. IMI has adapted an OCT setup to a rotary clamp elongational rheometer that uses counter-rotating belts to stretch a polymeric material in the molten state. Elongational flow properties of polymers are relevant to industrial processes such as film blowing and foam extrusion. In this apparatus, the specimen is subjected to a uniaxial deformation under a constant strain rate. It asks for precise monitoring, in real-time, of the volume of the sample. Since the length of the sample studied is fixed, only the width and thickness of the sample need to be monitored. IMI has modified the elongational rheometer to measure the positions of the upper and lower surfaces of the sample using OCT. By scanning in a transverse direction with a galvanometer-mounted mirror, the width is also obtained. OCT is very well suited for this task since many polymeric materials are translucent to visible and near-infrared light. OCT is also non-contact and can easily be applied to a sample heated at a few hundred degrees Celsius as in the case of a Polymer Melt Elongational Rheometer for Melts. The modified rheometer provides more accurate results (an order of magnitude) in real-time and is particularly useful when the sample thickness gets in the 100 µm range just before it breaks.

4. SPECKLE TO DIFFERENTIATE TISSUES

Imaging of a biological tissue with OCT provides an image that contains a well developed speckle structure. Speckle in OCT is usually described as resulting from two contributions: the multiple backscattering processes that occur within the volume defined by the coherence length and the spot size at a given depth, and the random delays related to multiple forward scattering in the medium. The first source is usually considered more important. The speckle is often seen as degrading the signal and there exists a wealth of literature about techniques to reduce speckle in OCT imaging. Both the nature of speckle and the speckle reduction techniques are reviewed in Ref. 5. A few papers attempt to rely upon information contained in the speckle pattern to differentiate biological tissues. Two main approaches have been studied. The first one relies on speckle contrast that has been shown to be quite sensitive to the number of scatterers contained within the probed volume.[6,7] Contrast is a simple parameter readily obtained from the first order statistics of speckle, it is defined by $C = <\Delta I^2>^{1/2} / <I>$, where I is the measured intensity. The limiting value of the contrast is 0.52 for a dense distribution of scatterers and it takes larger values when the number of scatterers is small. Since one expects normally a large amount of scatterers in biological tissues, authors of Ref. 7 suggest that this technique should be of

interest in high-resolution OCT where the probed volume is smaller. In a second approach, the authors of Refs. 6 and 8 rescale the measured intensity in the OCT images and use established texture analysis techniques to characterize the speckle pattern while relying on a classification algorithm to differentiate various tissue phantoms. This relies on two-dimensional statistics. Obtained results are encouraging, although they are strongly dependent upon the samples studied and the experimental setup used. All these approaches are in fact strongly sensitive to the optical setup used. For example, in contrast measurements, the probed volume, which is defined by the coherence length and the spot size, increases away from the focal plane since the spot diameter increases. Consequently, the number of scatterers contained in the probed volume also increases and the contrast decreases. For texture measurements, the effect of the optical setup on the measured parameters is also present, although it is more difficult to describe in a simple way its effect on the various texture measurements, especially since the image intensity is rescaled before treatment.

In this section, we present initial results from our contribution to the identification of tissue properties from the speckle pattern by looking at the variation of other parameters with changes in the density of scatterers. We first focus on speckle dimensions, both transverse and axial, and then look at an additional parameter extracted from the autocorrelation of the speckle pattern. Axial speckle size is mainly determined by the light source characteristics while transverse speckle size is related to the focusing optics. Interference resulting from combining the interferograms from the multiple scatterers contained within the probed volume will affect the observed speckle size. Our final goal is to identify the combination of parameters that would provide a robust index to differentiate tissues or materials while taking into account the coherence properties of the source, the focusing optics, and the distance from the focal plane where the measurement is done.

To begin this analysis, a model was developed to simulate the creation of the speckle pattern in an OCT system. Gaussian beam propagation of incoming light in the sample arm is described using the ABCD matrix formalism[9] and the backscattered light from each scatterer is treated as a spherical wave also retropropagated in the optical system with the ABCD matrix formalism. The tissue is modeled by various densities of punctual scatterers randomly distributed in a 3D volume.

We rely on the same definition of the effective number of scatterers (ENS) in the probed volume as in Ref. 7 to differentiate the samples. It corresponds to the number of scatterers in a volume defined by the spot size diameter D ($1/e^2$ criteria for intensity) and the length L defined by $L = l_c / n$ where n is the refractive index. The expression for the coherence length l_c used in Ref. 7 is provided in Ref. 10 and takes the form $l_c = \sqrt{2\ln(2)/\pi}\,\lambda^2 / \Delta\lambda$ where $\Delta\lambda$ is the full-width at half-maximum of the source wavelength bandwidth.

To validate the model, Fig. 2 presents an excellent agreement between the model (continuous line) and experiment (dashed line) for a liquid phantom similar to those used in Ref. 7 (one micron polystyrene spheres dissolved in water). Measurement was performed with our in-house OCT system using a Covega supraluminescent diode centered at 1310 nm with a bandwidth of about 65 nm. The whole OCT system is fibered, uses a common-path configuration, and relies on balanced detection. The light is delivered to the sample arm with an SMF-28 monomode fiber, collimated and focused in the sample. The beam is Gaussian with a spot size of 5.4 microns ($1/e^2$ for intensity). Athough the theoretical
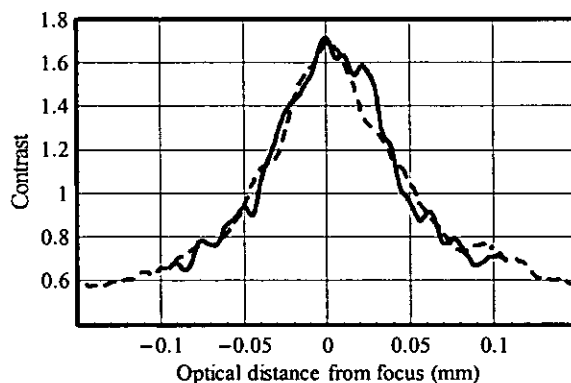

Fig. 2. Comparison between model and experiment of the contrast as a function of the position relative to the focal plane (0 mm) for 1 micron polystyrene spheres in water. The ENS value at the focal plane is 0.45.

OCT full-width at half-maximum (FWHM) resolution is expected to be 12 microns in air using the source parameters, experimental characterization of the system shows that the resolution is more of the order of 14 microns in air. Consequently, the value of L is evaluated to 16 microns. In Ref. 7 one finds modeling of the speckle contrast for a given probed volume, our model is more general since it includes the variation of the probed volume with depth. The horizontal axis in Fig. 2 represents the optical distance from the focal plane ($n\,d$, where n is the refractive index and d the geometrical distance). Near the focal plane (around 0 mm in Fig. 2), the ENS value is 0.45 thus leading to rather high contrast value. Away from the focal plane, the spot size increases, so does the ENS value, leading to a decrease in measured contrast. At 100 microns either side of the focal plane, the spot size is 3.4 times larger, leading to an ENS value of 5.2, with a quite reduced contrast.

The speckle size can be estimated from the Fourier transform or from the autocorrelation of the speckle pattern. In the following, we use the full-width at half-maximum to characterize the speckle size both in the axial and transverse directions. Fig. 3a presents the variation in speckle size in both directions as a function of the ENS value in the focal region as estimated by the model. These values are obtained from the simulation of an OCT measurement over a 1 mm transverse direction with a 1 micron step and an axial optical distance of +/- 100 microns from the focal plane. The envelope of the OCT signal is used. The simulated OCT system has a resolution of 12.6 microns in air and the focal spot diameter D is 5.4 microns ($1/e^2$ for intensity). The medium considered is water. The axial speckle size is evaluated from the autocorrelation of the speckle pattern evaluated with a kernel of 50 microns around the focal plane and averaged for all A-scans. It corresponds to the OCT resolution in air (12.6 microns) for small values of ENS and decreases with increasing values of ENS. The transverse speckle size is evaluated from the Fourier transform of the speckle pattern evaluated for each depth over the full transverse measurement width and then averaged over an axial optical distance of 50 microns around the focal plane. It corresponds to $D\sqrt{Log(2)/2}$ for small values of ENS and decreases also for larger values. The transverse speckle size is smaller than the spot size D in the focal region due to the retro-propagation of light in the focusing optics and also due to the fact that we consider the FWHM instead of the $1/e^2$ criterion.

Figure 3b presents the variation of the transverse speckle size as a function of the optical distance from the focal plane for various ENS values at the focal plane. It is again evaluated from the Fourier transform of the speckle pattern. Away from the focal plane, the speckle size is expected to increase since the spot size increases. But the effective number of scatterers in the probed volume also increases, which contributes to reduce the transverse speckle size. The competition between these two contributions is apparent for ENS=1.5 case, for which the transverse size begin to increase away from the focal plane and then decreases for distances larger than 50 microns.

Another interesting parameter may be obtained from the autocorrelation of the speckle pattern. The presence of many diffusers leads to a background level in the autocorrelation and this background is related to the density of diffusers. We have fitted the central peak of the transverse autocorrelation with $A\exp(-x^2/c^2)+B$ and Fig. 4 presents the ratio $B/(A+B)$ for various values of ENS at the focal region as a function of the distance from the focal plane. This ratio, which is quite sensitive to the density of scatterers, provides information somewhat similar to the contrast.
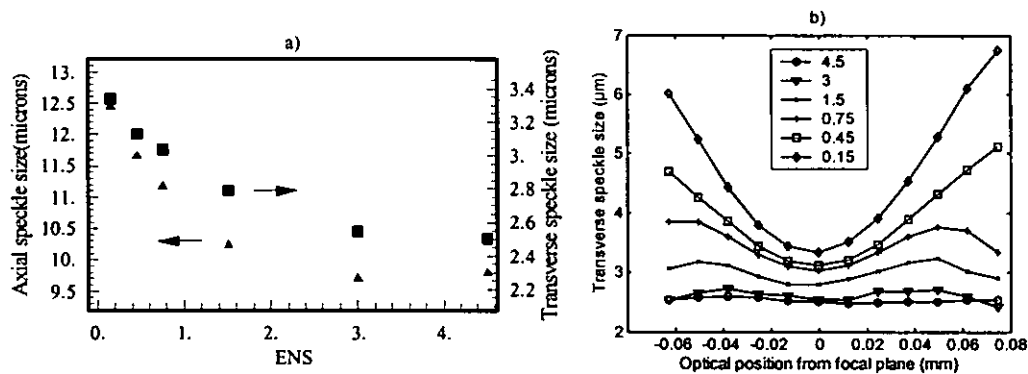

Fig. 3. a) Axial and transverse speckle dimensions as a function of the effective number of scatterers in the focal region and b) variation of the transverse speckle size with optical distance (distance times the index of refraction) from the focal plane for samples characterized by different ENS values in the focal region.

Fig. 4. Variation of the ratio B/(A+B) evaluated from the transverse autocorrelation with optical distance (distance times the index of refraction) from the focal plane for samples characterized by different ENS values in the focal region.
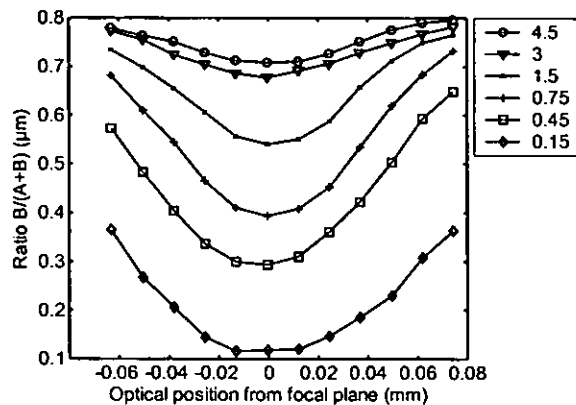
5. CONCLUSION

Activities in low-coherence tomography and low-coherence interferometry at the Industrial Materials Institute were reviewed. Preliminary results of a joint effort with Ecole Polytechnique of Montreal to identify speckle properties for the identification of tissues and materials were presented. The speckle transverse and axial dimensions are quite sensitive to variations in the density of scatterers when a few scatterers are contained within the probed volume. Additional information from the autocorrelation of the speckle pattern was also shown to be quite sentitive to the density of scatterrers. Current work includes the realization of solid phantoms to validate the modeled variations experimentally. It also includes the investigation of additional parameters related to speckle and the integration of all relevant parameters to perform a robust and efficient differentiation of biological tissues and industrial materials from the speckle pattern measured in OCT.

REFERENCES

1. A. M. Rollins, and A. Izatt Joseph, "Reference Optical Delay Scanning," in Handbook of Optical Coherence Tomography, B. E. Bouma, and G. J. Tearney, eds. (Marcel Dekker, New-York, 2002), pp. 99-123.
2. K. F. Kwong, D. Yankelevich, K. C. Chu, J. P. Heritage, and A. Dienes, "400-Hz mechanical scanning optical delay line," Optics Letters 18, 558-560 (1993).
3. G. J. Tearney , B. E. Bouma, and J. G. Fujimoto , "High-speed phase- and group-delay scanning with a grating based phase control delay line", Optics Letters 22, 1811-1813 (1997).
4. M. L. Dufour, G. Lamouche, V. Detalle, B. Gauthier, and P. Sammut, "Low-coherence interferometry - an advanced technique for optical metrology in industry," Insight 47, 216-219 (2005).
5. J. M. Schmitt, S.H.Xiang, and K.M Yung, "Speckle reduction techniques," in Handbook of Optical Coherence Tomography, B. E. Bouma, and G. J. Tearney, eds. (Marcel Dekker, New-York, 2002), pp. 175-199.
6. T. S. Tkaczyk, K. W. Gossage, and J. K. Barton, "Speckle image properties in optical coherence tomography," Proceedings of the SPIE The International Society for Optical Engineering 4619, 59-70 (2002).
7. I. T. R. Hillman, S. G. Adie, V. Seemann, J. J. Armstrong, S. L. Jacques, and D. D. Sampson, "Correlation of static speckle with sample properties in optical coherence tomography," Optics Letters 31, 190-192 (2006).
8. I. K. W. Gossage, C. M. Smith, E. M. Kanter, L. P. Hariri, A. L. Stone, J. J. Rodriguez, S. K. Williams, and J. K. Barton, "Texture analysis of speckle in optical coherence tomography images of tissue phantoms," Phys Med Biol 51, 1563-1575 (2006).
9. A. E. Siegman, Lasers (University Science Books, 1986)
10. D. D. Sampson and T. R. Hillman,"Optical Coherence Tomography," in Lasers and Current Optical Techniques in Biology, G. Palumbo and R. Pratesi, eds. (Royal Society of Chemistry, 2004).